Journal of Critical Reviews

ISSN- 2394-5125 Vol 7, Issue 4, 2020

Review Article

MODELLING OF WELDING PARAMETERS ON BEAD GEOMETRY IN ND: YAG LASER WELDING OF TITANIUM WITH TI-6AL-7NB USING RESPONSE SURFACE (RSM)

[1]Weaam Mohammed Moslim,[2]Jassim M. Salman,[3]Saad Hameed Al-Shafaie

College of Materials Engineering, University of Babylon, Iraq

Correspondence author: Weaam Mohammed Moslim mohamad_eng51@yahoo.com .

Received: 22.12.2019 *Revised: 24.01.2020* *Accepted: 26.02.2020*

Abstract

Pulsed laser welding is a powerful technique especially suitable for joining thin sheet metals. In this study, based on experimental data, pulsed laser welding of thin Cp- Ti and Ti-6Al-7Nb sheets has been optimized. The experimental data required for modeling are gathered as per Central Composite Design matrix in Response Surface Methodology (RSM) with full replication of 30 runs. Response Surface Methodology is used to investigate the effect of four input variables, namely: type of workpiece (WP), pulse energy (PE), pulse duration (T_{on}), welding speed (WS) and on the depth of penetration and bead width in YAG laser welding process. To study the proposed second-order polynomial model for DOP and BW, a Central Composite Design is used for estimating the model coefficients of the four input factors on DOP and BW. Experiments were conducted on Cp- Ti alloy with Ti-6Al-7Nb alloy. The significant coefficients are obtained by performing an Analysis of Variance at the 5 % level of significance. The results revealed that DOP and BW are more influenced by type of workpiece, pulse energy, pulse duration, welding speed and few of their interactions. A mathematical regression model was developed to predict both of DOP and BW in YAG laser welding. Also, the developed model could be used for the selection of the levels in this process for saving in welding time.

Keywords: Pulsed Nd- YAG laser welding, Ti, Ti-6Al-7Nb alloy, Bead Geometry(DOP&BW), Modelling and RSM.

DOI: http://dx.doi.org/10.31838/jcr.07.04.22

INTRODUCTION

Titanium and titanium alloys are widely used in space, aerospace, ship and chemical, nuclear energy and medical industries, because of many advantages such as low specific weight, high strength, excellent corrosion resistance, attractive fracture behavior and high melting point. Weldability of commercial pure titanium and most titanium alloys is good in general, although special cares must be taken during the welding process because pure titanium and titanium alloys are highly susceptible to contamination from atmospheric gases [1]. Joining two dissimilar metals is often difficult due to the distinct material properties and chemical reactions between different materials which can lead to the formation of intermetallic compounds (IMC) at the metals interface during the welding process. The presence of IMC in weld joints generally degrades the mechanical properties and quality of the welds. Therefore, the effort during the design of technology for welding of dissimilar material is aimed at elimination of IMC formation. The thickness of the IMC layer depends on the temperature profile generated by the heat source exploited for welding and the heat flux distribution across the interface. However, the thermal fields are also responsible for geometry of the fusion zone and thus the dimension of the bonding area[2]. Laser beam welding (LBW) is widely used manufacturing process for welding of similar and dissimilar materials. Narrow heat affected zone and lower distortion are the key feature of LBW, compared to the conventional welding. It is a widely growing technology due to its very smooth, precise and effective operation. The amount of heat input used in LBW is comparable to that of conventional joining processes. The weld pool developed in laser welding is smaller compared to arc welding process. The specific feature of LBW of high energy density and greater welding speed reduces the thickness of reactive interlayer and restricts the formation of intermetallic phase during dissimilar joining of materials[1]. The LBW are of two types based on energy transfer mode and depth of penetration, namely conduction and keyhole welding[3]. Moreover, the capital cost of laser welding is significantly higher than the traditional fusion processes although it can be compensated with high and excellent joint quality. Under optimized processing conditions, the static strength of the laser-welded titanium alloy samples can be close to the original material; however, there are still some processing problems such as lower elongation and corrosion resistance coupled with inferior fatigue properties[4]. The microstructures of α + β titanium alloys play an important role in determining the mechanical properties and fracture behavior of these materials[5]. The weld pool dimensions and weld quality of spot welds produced using a pulsed Nd: YAG laser welding machine depend on various process parameters including the spatial intensity distribution of the incident laser beam, the peak power of the pulse, the pulse energy, the pulse time, and the temporal shape of the beam power during the pulse. When developing a welding procedure for a specific application, each of these parameters must be characterized and fully specified[6]. Nowadays, laser beam is applied for the various processes like heat treatment, material removal, alloying, cladding, cutting, drilling and welding. Among all these processes, laser welding is considered as widely recommended process for the joining of similar/dissimilar metals. Laser beam welding is a welding process used to join two metals by the use of a laser source. The laser source provides intense and high density heat source, allowing for narrow, deep weld bead with high welding scan speed, now-a-days it has wide applications in various metal working industries due to its advantageous effects over other machining operations. Laser beam welding has high power density and a small heat affected zone due to high heating and cooling rates. Laser beam welding is a versatile process, which can weld almost all materials including aluminum, titanium, carbon steels, HSLA steels and stainless steel. The laser beam is an efficient technique to join different metals. This can join metals at the surface level and also at depth and produce very strong welding. It can be coupled with conventional welding processes to give required weld quality. The laser welding offers many features which make it an attractive alternative to conventional processes. Continuous or pulsed laser beam may be used depending upon the various applications in metal industries. Thin materials are welded by millisecond-long

pulses while continuous laser systems are used for deep welds. The laser welding process operates at very high scan speeds with low deformation as intense energy beam of light is used as heat source. Since it requires no filler material, laser welding reduces costs [7-9].

In the present work, firstly RSM is employed to development of mathematical models. The second aim is to find the optimal welding combination that would maximize the penetration depth while minimizing other bead geometry (welded zone width, heat affected zone width, welded zone area and heat affected zone area) with examine the welding parameters viz. pulse energy (PE), pulse on time (Ton) and welding speed (WS) on the depth of penetration (DOP) and bead width (BW) in Laser Nd: YAG of Titanium with Ti-6Al-7Nb Alloys and modelling of the execution measures by means of response surface methodology (RSM).The laser-welding parameters used in this study were parameters that can be controlled on the welding machine.

EXPERIMENTAL WORK

Experimental was carried out on commercial purity titanium (Ti) and Ti-6Al-7Nb with 100 × 50 mm and 1.5 mm thickness. The major chemical composition and mechanical/physical properties of this alloys are listed in Table 1.

In the present investigation, all the experiments were performed on Pulse Nd-YAG laser welding as a source of laser (model Haas HL3006D), accompanied with high speed imaging (HIS), this laser is able to radiate a continuous wave mode (this mode was actually used in the experiments) with up to 3KW and predetermined were recorded using a high speed imaging system. Fig. 1 show the employed laser system.

Table 1: Chemical composition of Ti and Ti-6Al-7Nb alloy used.

Element	Ti	Ti-6Al-7Nb
Al	<0.005	7.0
V	0.011	<0.01
Cr	<0.005	<0.005
Cu	0.005	0.01
Fe	0.15	0.06
Mn	<0.005	0.02
Mo	<0.01	0.03
Nb	0.01	4.46
Sn	<0.02	<0.02
Ni	<0.005	0.005
Si	0.01	0.03
Zr	0.02	0.04
Pd	<0.01	<0.01
Ru	<0.01	0.01
Ti	Base	Base

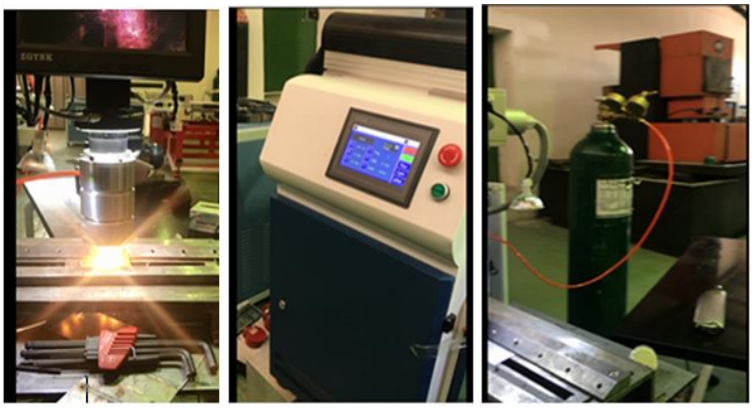

Fig. 1: show the Pulse Nd: YAG laser welding system, (a) laser welding machine; (b) laser generating device and (c) argon gas tube.

A coaxial nozzle is used purging pure argon gas (purity 99.998) with the laser beam. The pulsed Nd: YAG laser has adjustable pulse shape which offers high flexibility in optimizing the weld parameters to achieve defect free joints.

RESPONSE SURFACE METHODOLOGY

Response surface methodology (RSM) is a combination of mathematical, statistical method and it can be used to develop the regression model and optimization of engineering problems [10]. It is one of the Design of Experiments method used to approximate an unknown function for which only a few values are computed. These relations are then modelled by using least square error fitting of the response surface. A Central Composite Design (CCD) is used since it gives a comparatively accurate prediction of all response variable averages related to quantities measured during experimentation [11]. CCD offers the advantage that certain level adjustments are acceptable and can be applied in the two-step chronological RSM. In these methods, there is a possibility that the experiments will stop with a few runs and decide that the prediction model is satisfactory.

In CCD, the limits of the experimental domain to be explored are defined and are made as wide as possible to obtain a clear response from the model. The WP, PE, Ton, and WS are the

welding variables selected for this investigation. The different levels taken for this study are depicted in Table 2. The arrangement to conduct the experiments using a CCD with four variables, the cardinal points used are sixteen cube points, eight axial points and six center point, in total of 30 runs in three blocks [12]. The values of DOP and BW are shown in Table 3.

The second-order model is normally used when the response function is not known or nonlinear. In the present study, a second-order model has been utilized. The experimental values are analyzed and the mathematical model is then developed that illustrate the relationship between the process variable and response. The second-order model in equation (1) explains the behaviour of the system [13].

$$Y = \beta o \sum_{i=1}^{k} \beta_i X_i + \sum_{i=1}^{k} \beta_{ii} X_i^2 + \sum_{i<j=2}^{k} \beta_{ij} X_i X_j \pm \varepsilon$$

Where Y is the corresponding response, Xi is the input variables, X²ii and XiXj are the squares and interaction terms, respectively, of these input variables. The unknown regression coefficients are βo, βi, βij and βii and the error in the model is depicted as ε.

Table 2: Input Variables used in the experiment and their levels.

Variable	*Unit*	Levels		
		-1	0	1
workpieces type WP	--	AA	AB	BB
pulse energy PE	*J*	9	12	15
pulse duration Ton	*μs*	4	6	8
welding speed WS	*mm/s*	3	5	7

A: Ti, B: Ti-6Al-7Nb, AA: Ti + Ti, BB: Ti-6Al-7Nb + Ti-6Al-7Nb, AB: Ti + Ti-6Al-7Nb.

Table 3: Design layout & experimental results. (CCD).

Run Order	Pt Type	Blocks	WP ---	PE J	Ton μsec.	WS mm /s	BW μm	DOP μm
1	1	1	-1	-1	-1	1	384	349
2	1	1	1	-1	-1	-1	731	542
3	1	1	-1	-1	1	-1	606	551
4	1	1	-1	1	-1	-1	627	570
5	1	1	1	1	-1	1	930	689
6	0	1	1	-1	1	1	900	666
7	1	1	0	0	0	0	747	623
8	0	1	0	0	0	0	748	624
9	1	1	-1	1	1	1	771	701
10	1	1	1	1	1	-1	1467	1086
11	0	2	0	-1	0	0	623	519
12	1	2	0	0	0	0	750	625
13	1	2	0	0	0	1	695	579
14	0	2	0	0	0	-1	787	656
15	1	2	0	0	-1	0	639	532

Table 4: Design layout & experimental results. (CCD)

Run Order	Pt Type	Blocks	WP ---	PE J	Ton μsec.	WS mm/s	BW μm	DOP μm
16	1	2	1	0	0	0	976	722
17	1	2	-1	0	0	0	581	528
18	1	2	0	0	1	0	890	741
19	1	2	0	0	0	0	749	624
20	1	2	0	1	0	0	897	747
21	0	3	-1	1	-1	1	554	503
22	-1	3	-1	-1	1	1	535	487
23	-1	3	0	0	0	0	748	626
24	0	3	-1	-1	-1	-1	435	396
25	-1	3	-1	1	1	-1	873	793
26	-1	3	1	-1	1	-1	1018	754
27	-1	3	1	1	1	1	1296	960
28	-1	3	1	1	-1	-1	1053	780
29	-1	3	1	-1	-1	1	646	478
30	-1	3	0	0	0	0	747	623

PtType 1 indicates a cube point of the design;
PtType 0 indicates a center point;
PtType -1 indicates an axial point;

The unknown coefficients are determined from the experimental data as presented in Table 4. The standard errors in the estimation of the coefficients are tabulated in the column 'SE cof.'. The F ratios are calculated for 95% level of confidence and the factors having p-value more than 0.05 are considered insignificant (shown with * in p-column). For the

appropriate fitting of DOP and BW, the non-significant terms are eliminated by the backward elimination process. The regression model is re-evaluated by determining the unknown coefficients, which are tabulated in Table 5. The model made to represent DOP and BW depicts that WP, PE, Ton, WS, E. WP^2, $PE^2 \times Ton^2$, WS^2, WP×PE, WP × Ton and PE × Ton are the most influencing parameters in order of significance. The final response equations for DOP and BW are given in equations (**2**) & (3) respectively.

BW = 747.42 + 202.83 × WP + 143.89 × PE + 130.94 × Ton – 49.22 × WS + 28.99 × WP2 + 10.49 × PE2 + 14.99 × Ton2 + 36.62 × WP × PE + 33.50 × WP × Ton – 12.50 × WP × WS + 23.75 × PE × Ton – 9.00 × PE × WS – 8.13 × Ton ×WS..... (2)

DOP = 623.53 + 99.944 × WP + 115.944 × PE + 105.556 × Ton – 39.778 × WS + 2.11 × WP2 + 10.11 × PE2 + 13.61 × Ton2 – 5.39 × WS2 + 18.19 × WP × PE + 16.44 × WP × Ton – 6.19 × WP × WS + 19.06 × PE × Ton – 7.06 × PE × WS – 6.31 × Ton × WS..... (3)

Table 5: Estimated Regression Coefficients for UTS (Before backward elimination).

	BW model			DOP model		
Term	Coef.	T-value	P-value	Coef.	T-value	P-value
Constant	747.87	286.17	0.000	623.53	485.71	0.000
WP	202.83	102.29	0.000	99.944	102.60	0.000
PE	143.89	72.56	0.000	115.944	119.03	0.000
Ton	130.94	66.03	0.000	105.556	108.36	0.000
WS	-49.22	-24.82	0.000	-39.778	-40.84	0.000
WP × WP	30.93	5.92	0.073*	2.11	0.82	0.423*
PE ×PE	12.43	2.38	0.031	10.11	3.94	0.001
Ton × Ton	16.93	3.24	0.006	13.61	5.30	0.000
WS × WS	-6.57	-1.26	0.228*	-5.39	-2.10	0.053*
WP × PE	36.62	17.41	0.912*	18.19	17.60	0.074*
WP × Ton	33.50	15.93	0.081*	16.44	15.91	0.811*
WP × WS	-12.50	-5.94	0.062*	-6.19	-5.99	0.105*
PE × Ton	23.75	11.29	0.071*	19.06	18.45	0.083*
PE × WS	-9.00	-4.28	0.081*	-7.06	-6.84	0.077*
Ton × WS	-8.13	-3.86	0.092*	-6.31	-6.11	0.065*
R^2	99.93			99.96		
$R^2_{adj.}$	99.87			99.93		
$R^2_{pred.}$	99.48			99.71		

Since, YAG laser welding process is non-linear in nature, a linear polynomial will be not able to predict the response accurately, and therefore the second-order model (quadratic model) is found to be adequately modelled the process. The ANOVA table for the curtailed quadratic model (Table 6) depicts the value of the coefficient of determination, R^2 as 99.93% and 99.96%, which signifies that how much variation in the response is explained by the model. The higher of R^2, indicates the best fitting of the model with the data.

The model adequacy checking includes the test for significance of the regression model, model coefficients, and lack of fit, which is carried out subsequently using ANOVA on the curtailed model (Table 6). The total error of regression is the sum of errors in linear, square, and interaction terms.

Table 6: Analysis of Variance for DOP and BW.

Source	DF	Adj SS	Adj MS	F	P
For BW					
Regression	13	1536535	118195	1611.48	0.000
Linear	4	1465464	366366	4995.08	0.000
WP	1	740544	740544	10096.67	0.000
PE	1	372672	372672	5081.06	0.000
Ton	1	308636	308636	4207.98	0.000
WS	1	43611	43611	594.60	0.000
Square	3	17776	5925	80.79	0.000
Ton × Ton	1	638	638	8.70	0.009
Error	16	1174	73		
Lack-of-Fit	11	1167	106	77.61	0.000
Pure Error	5	7	1		
Total	29	1537709			
For DOP					
Regression	13	671033	51618	2492.55	0.000
Linear	4	650813	162703	7856.68	0.000
WP	1	179800	179800	8682.27	0.000
PE	1	241976	241976	11684.65	0.000
Ton	1	200556	200556	9684.52	0.000
WS	1	28481	28481	1375.30	0.000
Square	3	2743	914	44.15	0.000

PE × PE	1	206	206	9.96	0.006
Ton × Ton	1	410	410	19.81	0.000
Error	16	331	21		
Lack-of-Fit	11	325	30	21.59	0.002
Pure Error	5	7	1		
Total	29	671365			

The residual error is the sum of pure and lack-of-fit errors. The fit summary recommended that the quadratic model is statistically significant for analysis of DOP and BW. In the table, P value for the lack-of-fit is 0.002 and 0.000 respectively, which are insignificant, so the model is certainly adequate. Moreover, the mean square error of pure error is less than that of lack-of-fit.

The final model tested for variance analysis (F-test) indicates that the adequacy of the test is established. The computed values of response parameters, model graphs are generated for the further analysis in the next section.

A complete residual analysis has been done for developing response and the graphs are shown in Fig. 3. Normal probability plot of residuals reveals that experimental data are spread approximately along a straight line, confirming a good correlation between experimental and predicted values for the response Fig.(3-a). In graph of residuals versus fitted values Fig. (3-b), only small variations can be seen. The histogram of residuals Fig. (3-c) also shows a Gaussian distribution which is desirable, and finally, in residuals against the order of experimentations in Fig. (3-d) both negative and positive residuals are apparent, indicating no special trend which is worthy from a statistical point of view. As a whole, all the yielded models do not show any inadequacy and so on in Fig. 4(a, b, c and d).

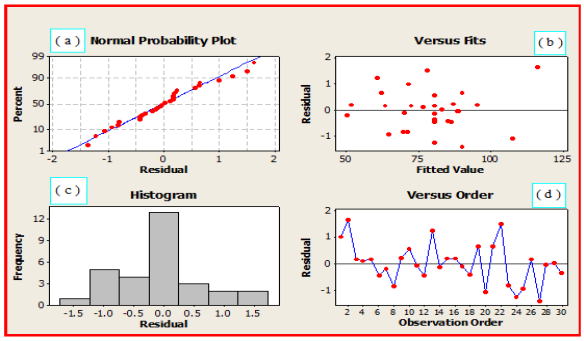

Fig. 3: Residual Plot for DOP.

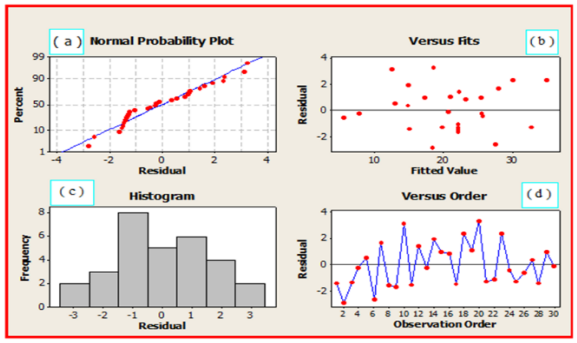

Fig. 4: Residual Plot for BW.

RESULT AND DISCUSSION

Fig. 4 and 5 depicts the main effect plots of the four controllable parameters on BW and DOP. Note that the effect of the four inputs on BW and DOP have the same behaviour also it is understandable that all variables have more influential impacts on BW and DOP. The results in the Table 6 support this.

More specifically, change in the workpiece type (from C.P. Ti to Ti-6Al-7Nb) alone, while keeping the other factors constant at their middle levels, can increase BW and DOP by 68% (581 µm to 976 µm) and 37% (528 µm to 722 µm) respectively. This can be explained by the low melting point of Ti-6Al-7Nb compared to C.P. Ti. This helps the laser beam to penetrate the low melting material (Ti-6Al-7Nb) more than the other (C.P. Ti) and thus increases BW and DOP. Also the responses BW and DOP increase when the PE and Ton increases by 44% for both and decreases by 11% and 12 % with WS increases.

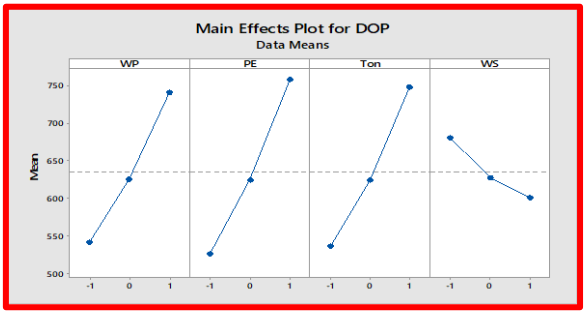

Fig. 5: Main effect plots for DOP.

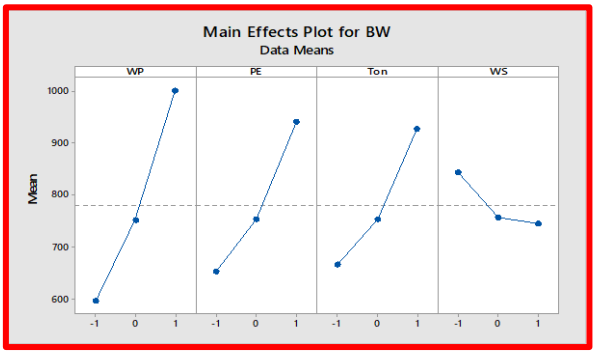

Fig. 6: Main effect plots for BW.

CONCLUSION

The following principal conclusions can be drawn:

1. As regards main effects analysis, changing WP from C.P. Ti to Ti-6Al-7NB and rising PE, Ton results in higher values of UTS whereas an increasing WS causes increase then decrease of UTS.
2. The factors input that significantly affected on the output responses (DOP and BW) were the WP, PE, Ton, and WS, WP^2, PE^2, Ton^2, WS^2, WP × PE, WP × Ton and PE × Ton with a confidence level of 95%.
3. The interaction effects of (WP × PE), (WP × Ton) and (PE × Ton) as well as all pure quadratic (square) have all been found to significantly control on both DOP and BW .
4. Though the Nd: YAG laser welding process parameters on Titanium alloys are highly interconnected due to its inherently complex and stochastic nature, however, the approach of RSM can beneficially help identifying process behaviour and determining appropriate Nd: YAG laser conditions meeting all performance criteria in a compromise manner.
5. All the main effects of input parameters, i.e., WP, PE, Ton, and WS were found to be highly significant in affecting the BW and DOP.

REFERENCES

1. Lisiecki Aleksander, 2012, "Laser Welding of Titanium Alloy TI6AL4V Using A Disk Laser", Welding Department of Silesian University of Technology, Poland, pp. 1-4.
2. MáriaBehúlová, EvaBabalová and MiroslavSahul, 2017, "Design of Laser Welding Parameters for Joining Ti Grade 2 and AW 5754 Aluminum Alloys Using Numerical Simulation", Advances in Materials Science and Engineering Volume 2017, Article ID 3451289, 15 pages.
3. Pramod Kumara and Amar Nath Sinhab, 2018, "Microstructure and mechanical properties of pulsed Nd:YAG laser welding of st37 carbon steel", Procedia Computer Science 133 (2018) 733–739.
4. S. T. Auwal, S. Ramesh, F. Yusof, and S. M. Manladan, 2018, " A review on laser beam welding of titanium alloys", The International Journal of Advanced Manufacturing Technology Procedia Engineering, 29 pages.
5. M. Y. Lu, L. W. Tsay and C Chen, 2012, " Notched Tensile Fracture of Ti-6Al-4V Laser Welds at Elevated Temperatures", Materials Transactions, Vol. 53, No. 6, pp. 1042 to 1047.
6. H. N. BRANSCH, D. C. WECKMAN And H. W. KERR, 1992, "Effects of Pulse Shaping on NchYAG Spot Welds in Austenitic Stainless Steel", Department of Mechanical Engineering, University of Waterloo, Waterloo, Ont., Canada, pp. 1-11.
7. Ceyhun K. and Engin K., 2017, "Robotic Nd: YAG Fiber Laser Welding of Ti-6Al-4V Alloy", 7, 221, pp. 1-11.
8. Nawi I.N., Saktioto, Fadhali M., Hussain M.S., Ali J. and Yupapin P.P. "Nd:YAG laser welding of stainless steel 304 for photonics device packaging", Procedia Engineering, Vol. 8, pp.374–379.
9. Sandeep S. S. and Sachin M., 2017, "Research Developments in Laser Welding - A Review", International Journal for Innovative Research in Science & Technology, Vol. 3, Issue 11, pp. 60-64.
10. Assarzadeh S. and Ghoreishi M., 2013, "Statistical modeling and optimization of the EDM parameters on WC-6%Co composite through a hybrid response surface methodology desirability function approach", International Journal of Engineering Science and Technology, Vol.5, No. 6, pp. 1279-1302.
11. Boopathi S. and Sivakumar K., 2014 "Study of water assisted dry wire-cut electrical discharge machining", Indian Journal of Engineering and Materials Science, Vol. 21, No. 1, pp. 75-82.
12. Mason R., Gunst R., Dallas, Texas and Hess J., 2003 "Statistical Design and Analysis of Experiments with Applications to Engineering and Science" Second Edition, A John Wiley & sons publication.
13. Minitab User Manual Release 16, 2013, MINITAB Inc, State College, PA, USA.
14. Kuni Zu'aimah Barikah. "Traditional and Novel Methods for Cocrystal Formation: A Mini Review." Systematic Reviews in Pharmacy 9.1 (2018), 79-82. Print. doi:10.5530/srp.2018.1.15
15. Saini, R., Saini, S., Sharma, S.Potential of probiotics in controlling cardiovascular diseases(2010) Journal of Cardiovascular Disease Research, 1 (4), pp. 213-214. DOI: 10.4103/0975-3583.74267